

---

# BISHOP MUSEUM OCCASIONAL PAPERS

---

TOOLS FOR  
RECONSTRUCTING  
HAWAIIAN FISH  
ASSEMBLAGES



BISHOP MUSEUM PRESS  
HONOLULU

---

Cover photo: Lateral aspect of the left, upper pharyngeal jaw of the parrotfish *Chlorurus perspicillatus* (Steindachner, 1879). Parallel lines indicate the limits of the length designated herein as Axis B (the distance between the fourth-epibranchial and cranial condyles). Scale bar = 1 mm..

## RESEARCH PUBLICATIONS OF BISHOP MUSEUM

Bishop Museum Press has been publishing scholarly books on the natural and cultural history of Hawai'i and the Pacific since 1892. The Bernice P. Bishop Museum Bulletin series (ISSN 0005-9439) was begun in 1922 as a series of monographs presenting the results of research in many scientific fields throughout the Pacific. In 1987, the *Bulletin* series was superceded by the Museum's five current monographic series, issued irregularly:

Bishop Museum Bulletins in Anthropology	(ISSN 0893-3111)
Bishop Museum Bulletins in Botany	(ISSN 0893-3138)
Bishop Museum Bulletins in Entomology	(ISSN 0893-3146)
Bishop Museum Bulletins in Zoology	(ISSN 0893-312X)
Bishop Museum Bulletins in Cultural and Environmental Studies	(ISSN 1548-9620)

Bishop Museum Press also publishes *Bishop Museum Occasional Papers* (ISSN 0893-1348), a series of short papers describing original research in the natural and cultural sciences.

To subscribe to any of the above series, or to purchase individual publications, please write to: Bishop Museum Press, 1525 Bernice Street, Honolulu, Hawai'i 96817-2704, USA. Phone: (808) 848-4135. Email: [press@bishopmuseum.org](mailto:press@bishopmuseum.org). Institutional libraries interested in exchanging publications may also contact the Bishop Museum Press for more information.

ISSN 0893-1348  
Copyright © 2011 by Bishop Museum



### BISHOP MUSEUM

The State Museum of Natural and Cultural History  
1525 Bernice Street  
Honolulu, Hawai'i 96817-2704, USA

## **Preface**

The original motivation for these two articles differed; however, both are useful for dietary analysis of the critically endangered, endemic, Hawaiian monk seal (*Monachus schauinslandi*). Food limitation is driving the unsustainable decline of monk seals in the Northwestern Hawaiian Islands, and because these studies will lead to a more thorough understanding of monk seal feeding, the Pacific Islands Fisheries Science Center (PIFSC, NOAA Fisheries) supported their publication. Researchers reconstructing Hawaiian fish assemblages may find complementary products supported by PIFSC useful.

To identify fishes based on their hard remains -

Dye, TS & KR Longenecker. 2004. Manual of Hawaiian Fish Remains Identification Based on the Skeletal Reference Collection of Alan C. Ziegler and Including Otoliths. *Society for Hawaiian Archaeology Special Publication* 1. 134 pp (CDROM). Available in two parts from the Society for Hawaiian Archaeology website: (<http://hawaiianarchaeology.org/bib/fish%20manual1.pdf>) & (<http://hawaiianarchaeology.org/bib/fish%20manual2.pdf>)

Longenecker, KR. 2011. Fish Remains: A tool for identifying Hawaiian fishes from bones, otoliths & scales. (<http://hbs.bishopmuseum.org/frc/>)

To reconstruct fish size from otoliths -

Longenecker, K. 2008. Relationships between otolith- and body-size for Hawaiian reef fishes. *Pacific Science* 62(4):533-539.





## Relationships between the length of select head bones and body weight for *Pseudanthias* (Serranidae: Anthiinae), numerically important prey of the endangered Hawaiian monk seal

KEN LONGENECKER (Hawaii Biological Survey, Bishop Museum, 1525 Bernice Street, Honolulu, Hawai'i 96817, USA; email: klongenecker@bishopmuseum.org)

Descriptions of the relationships between the size of durable structures (*e.g.*, bones) and the size of the organism that produced them are useful for describing past events. Examples include reconstructing diets from stomach contents, fecal or regurgitate samples, or middens; patterns of prehistoric human resource use from archaeological sites; and ancient communities from paleontological deposits (Longenecker, 2008).

Small-bodied anthiine serranids of the genus *Pseudanthias* have recently been found in the diet of the critically endangered Hawaiian monk seal (Longenecker, 2010). Numerically, these fishes are the overwhelmingly dominant prey of a sub-population of seals recently established in the main Hawaiian Islands, with as many as 886 individuals recovered from a single fecal sample (Cahoon, 2011). However, because of their small size, these fishes may not be an energetically important part of the diet. Equations that allow total body weight to be estimated from the size of prey remains will help resolve the importance of *Pseudanthias* in the monk seal diet. This will ultimately help inform conservation decisions for an apparently food-limited marine mammal.

Here I present the results of regression analyses examining the relationship between the dimensions of select head bones and the total body weight of *Pseudanthias* specimens. Because species-level identification of *Pseudanthias* remains recovered from monk seals has not been achieved, the equations are based on data from several species and are intended to represent Hawaiian members of the genus. The bones included in the analyses are those that have proven useful for identifying *Pseudanthias* remains (Longenecker, 2010; Cahoon, 2011) and have consistently yielded the highest estimates of minimum number of individuals in fecal samples.

### Materials and Methods

Thawed, previously frozen specimens of three *Pseudanthias* species collected from the Au'au Channel were measured (total, fork, and standard lengths) and weighed. The number and size range of each species is presented in Table 1. The majority of scales, skin, viscera, and muscle was manually removed from each specimen. Carcasses were then

**Table 1. *Pseudanthias* Specimens Examined.**

Species	N	Range (mm fork length)
<i>Pseudanthias bicolor</i>	1	100
<i>Pseudanthias hawaiiensis</i>	13	33–88
<i>Pseudanthias thompsoni</i>	5	32–69

dried in air to a jerky-like consistency, and placed in a culture of dermestid beetles to remove additional non-calcareous tissue. Resulting skeletons were soaked in water until disarticulated, then individual bones were cleaned with stiff-bristled brushes and air-dried. Specimens were deposited in the Bishop Museum faunal reference collection.

Dimensions of select head bones were measured with an ocular micrometer fitted to a dissecting microscope. Images of the bones examined and axes measured are presented in Figures 1–7 (terminology from Rojo, 1991). Regression analysis (2-parameter power function) was used to describe the relationship between bone size and total body weight. For paired bones (dentary, angular, maxilla, hyomandibular, preopercle, opercle), axes of both bones were measured and mean lengths were compared with a paired t-test. The mean of measurements from right and left bones from a single individual was used in regression analyses when no significant difference in axis length was detected between sides, otherwise side-specific equations were generated (dentary axis “B” and preopercle axis “B”).

### Results and Discussion

All regression equations presented in Table 2 explain a high percentage of variation in the data ( $r^2 \geq 0.840$ ) and should permit accurate estimates of the total body weight of individual *Pseudanthias* from the dimensions of select head bones. Of all bone axes examined, only the length of parasphenoid axis B was not adequately predictive of body weight. Because of its low  $r^2$  value (0.583) that regression equation is not presented.

Figures 8–14 show regression curves in relation to axis-length-to-body-weight scatterplots for each bone. These are intended to allow users of the regression equations in Table 2 to judge whether extrapolation is appropriate, or whether some equations may provide more-accurate weight predictions within certain bone size ranges.

Because some investigators may be interested in reconstructing fish lengths, and because length-weight relationships are basic information needs for fishery modeling, a

**Table 2. Relationships Between Bone Dimensions (x) in mm and Total Body Weight (y) in g.**

Bone, Axis (side)	Equation	N	$r^2$
Dentary, A	$y = 10.1616(x)^{1.5485}$	18	0.920
Dentary, B (left)	$y = 0.0459(x)^{2.7365}$	17	0.935
Dentary, B (right)	$y = 0.0305(x)^{2.9201}$	17	0.947
Angular	$y = 0.0202(x)^{3.1806}$	18	0.938
Maxilla	$y = 0.0014(x)^{3.9132}$	18	0.916
Hyomandibular, A	$y = 0.0173(x)^{3.2343}$	15	0.965
Hyomandibular, B	$y = 1.2695(x)^{1.5400}$	17	0.846
Preopercular, A	$y = 0.1686(x)^{2.2809}$	19	0.840
Preopercular, B (left)	$y = 0.0198(x)^{2.7939}$	18	0.875
Preopercular, B (right)	$y = 0.0121(x)^{3.0685}$	14	0.963
Opercular, A	$y = 0.0053(x)^{3.5695}$	17	0.944
Opercular, B	$y = 0.0139(x)^{3.2066}$	18	0.945
Parasphenoid, A	$y = 2.6025 \cdot 10^{-5}(x)^{5.0841}$	11	0.952

**Table 3. Length-weight and length-length regressions.**

Equation	N	r <sup>2</sup>
Wt = 2.1970 · 10 <sup>-6</sup> (FL) <sup>3.4890</sup>	19	0.986
SL = -1.2106 + 0.8523(FL)	19	0.992
TL = -16.6347 + 1.5094(FL)	16	0.902
TL = -11.2361 + 1.7167(SL)	16	0.850

Wt – weight (g); SL – standard length (mm); FL – fork length (mm); TL – total length (mm).

series of length-weight and length-length relationships are presented in Table 3. These will allow the conversion of any length or weight measurement or estimate into any other.

### Acknowledgments

I thank the following people for their help: Mandy Wong suggested which bones and axes to analyze; Harold Haga prepared skeletal specimens; Terry Lopez and Pumehana Imada produced bone images; Lydia Garetano produced images of and measured bones. Specimen collection was funded by the National Oceanic and Atmospheric Administration (NOAA) Coastal Ocean Program under award NA07NOS4780188 to the Bishop Museum, NA07NOS4780187 and NA07NOS478190 to the University of Hawaii, and NA07NOS4780189 to the State of Hawaii; and submersible support provided by NOAA Undersea Research Program's Hawaii Undersea Research Laboratory. Specimen preparation/measurement and manuscript preparation/publication was supported by contract AB133F-06-CN-0139 with the Protected Species Division of the Pacific Islands Fisheries Science Center (NOAA/NMFS). Figures 1–6 were produced on an Automontage<sup>®</sup> system funded by the National Science Foundation under Grant Number DEB-082868.

### Literature Cited

- Cahoon, M.K.** 2011. The foraging ecology of monk seals in the main Hawaiian Islands. Unpublished MS Thesis. University of Hawai‘i at Manoa, Honolulu. 172 pp.
- Longenecker, K.** 2008. Relationships between otolith size and body size for Hawaiian reef fishes. *Pacific Science* **62**: 533–539.
- . 2010. Fishes in the Hawaiian monk seal diet, based on regurgitate samples collected in the Northwestern Hawaiian Islands. *Marine Mammal Science* **26**: 420–429.
- Rojo, A.L.** 1991. *Dictionary of evolutionary fish osteology*. CRC Press, Boca Raton, Florida. 273 pp.

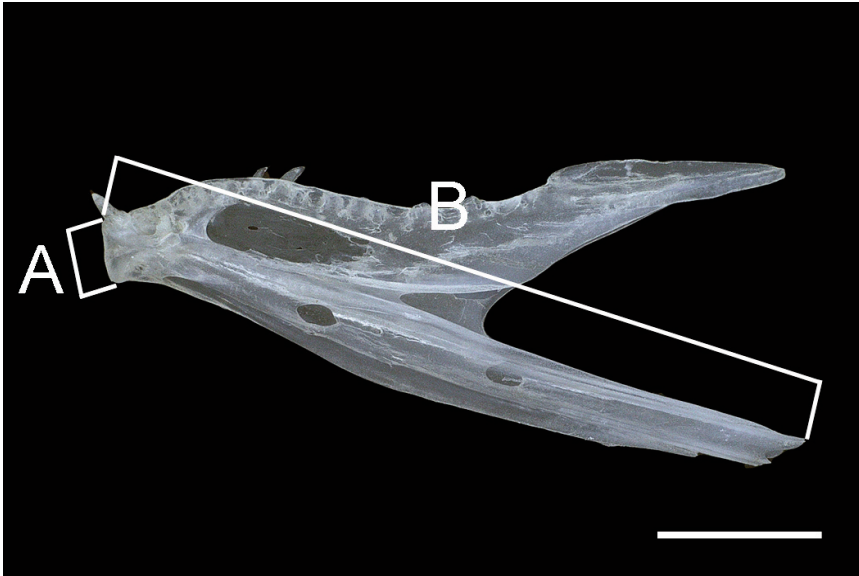


**Figure 1.** Axes measured on dentary (lateral aspect): A – height of mandibular symphysis; B – greatest distance between dorsal limit of mandibular symphysis and ventral process. Specimen: FR BPBM 0529, *Pseudanthias thompsoni*, 43.5 mm standard length. Scale bar = 1 mm.

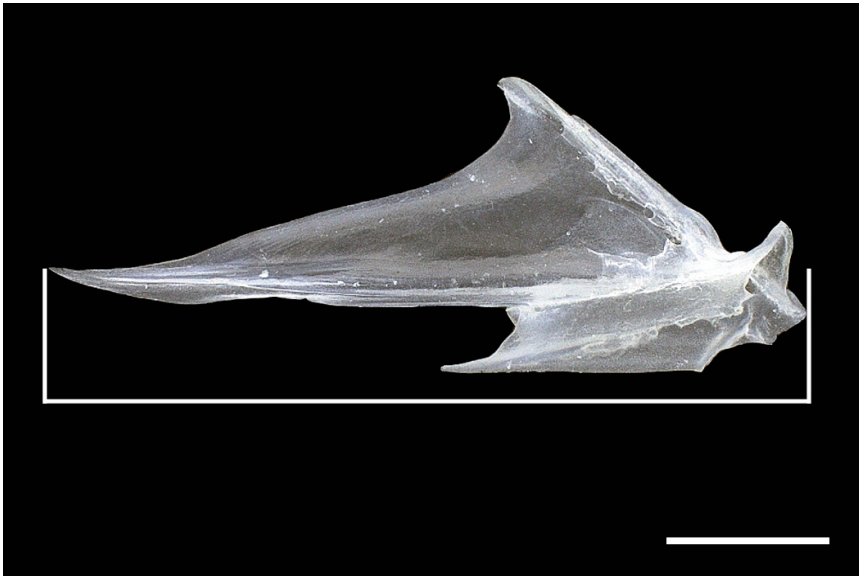


**Figure 2.** Axis measured on angular (lateral aspect): greatest distance along bone, beginning at anterior limit of anterior process. Specimen data as in Figure 1. Scale bar = 1 mm.

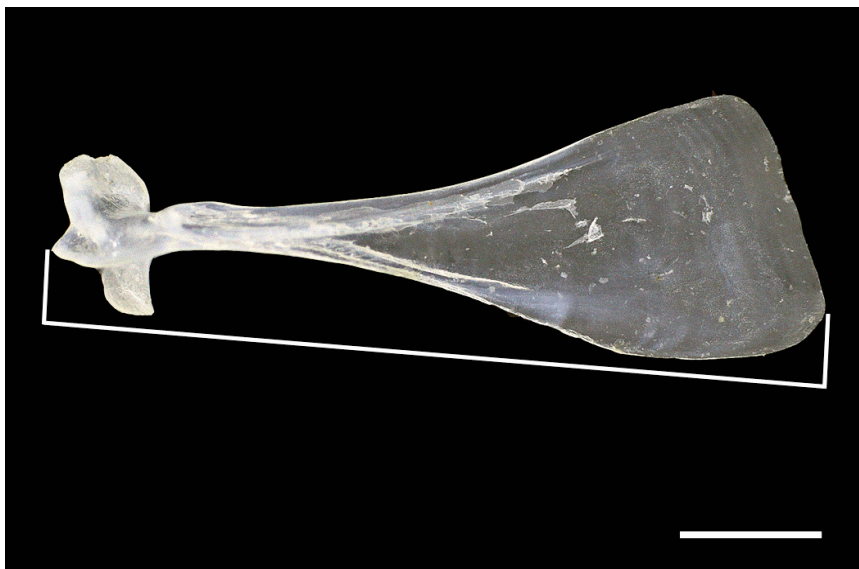


**Figure 3.** Axis measured on maxilla (lateral aspect): distance between the anterior limit of external process and posterior limit of caudal process. Specimen data as in Figure 1. Scale bar = 1 mm.

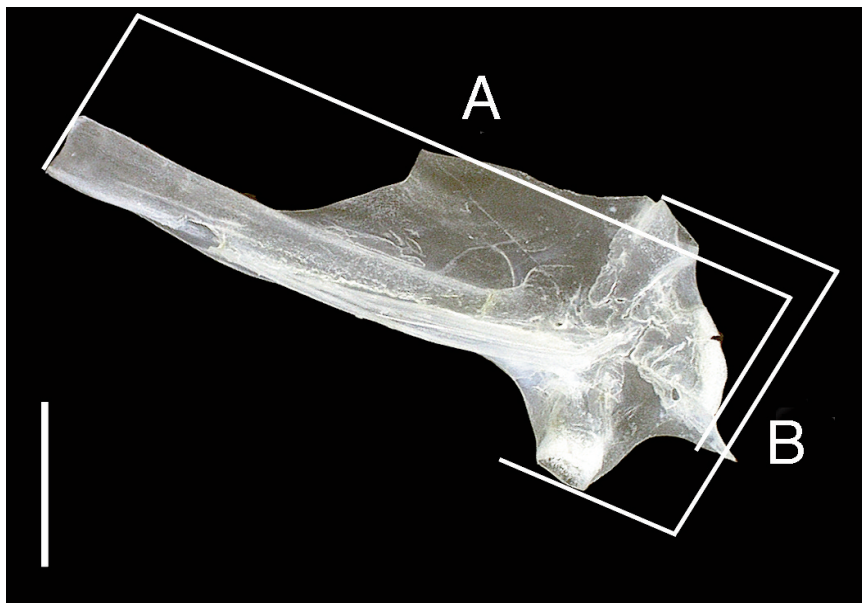


**Figure 4.** Axes measured on hyomandibular (lateral aspect, rotated 90° clockwise from its anatomical position): A – greatest distance between symplectic and pterotic facets; B – greatest distance between sphenotic facet and opercular process. Specimen data as in Figure 1. Scale bar = 1 mm.

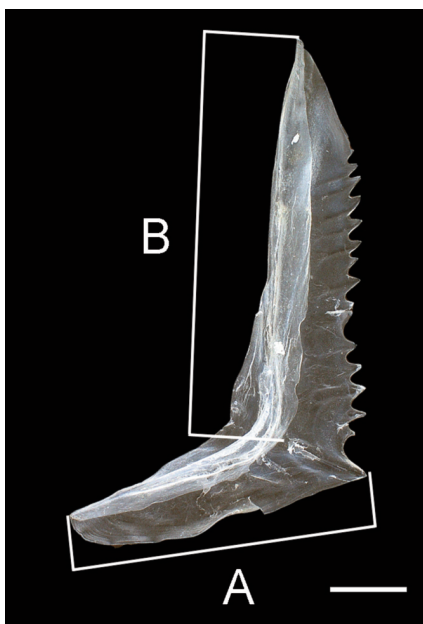


**Figure 5.** Axes measured on preopercle (lateral aspect): A – distance between anterior limit of quadrate crest and angle of posterior wing; B – distance between upper angle and free edge of sensory canal at its angle. Specimen data as in Figure 1. Scale bar = 1 mm.

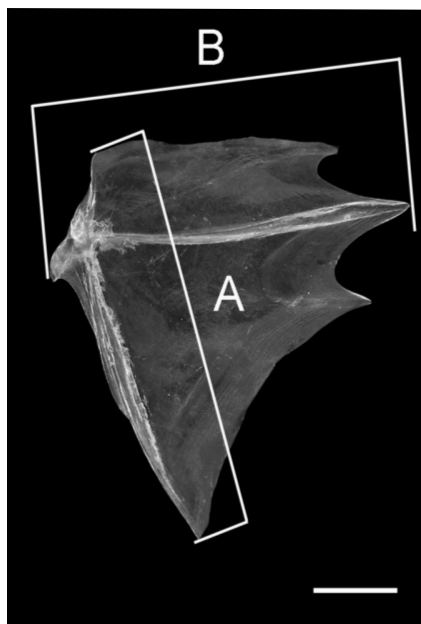


**Figure 6.** Axes measured on opercle (lateral aspect): A – distance between anterior limit of dorsal margin and inferior angle; B – distance between middle opercular spine and anterior limit of anterior margin near articular fossa. Specimen data as in Figure 1. Scale bar = 1 mm.

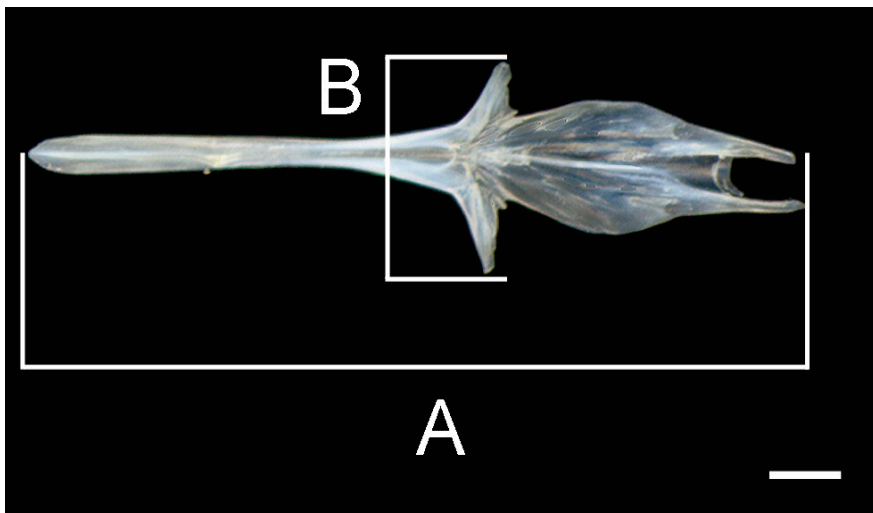


**Figure 7.** Axes measured on parasphenoid (ventral aspect): A – greatest distance along bone, beginning at anterior limit of anterior process; B – distance between lateral limits of alar processes. Specimen: FR BPBM 0526, *Pseudanthias thompsoni*, 56 mm standard length. Scale bar = 1 mm.

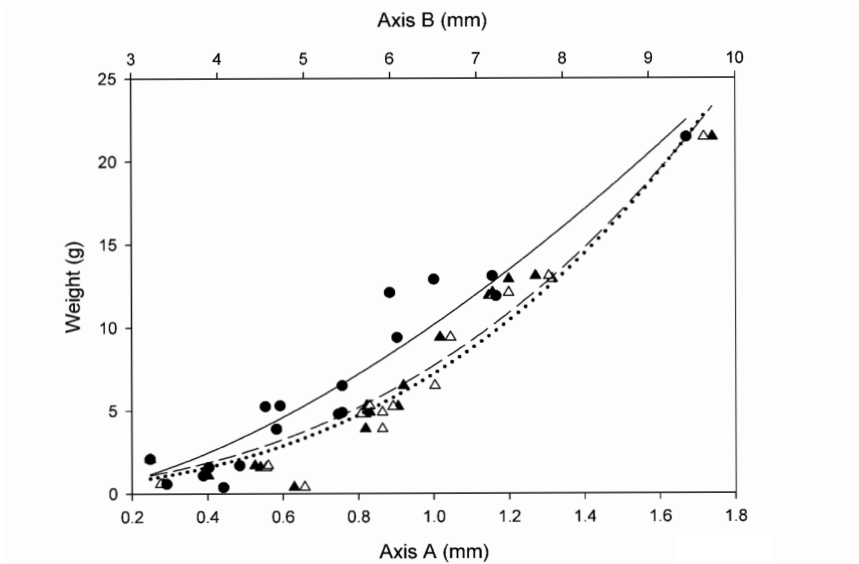


**Figure 8.** Relationships between dentary axis lengths and total body weight. A – circles, solid curve; B (left) – closed triangles, dashed curve; B (right) – open triangles, dotted curve.

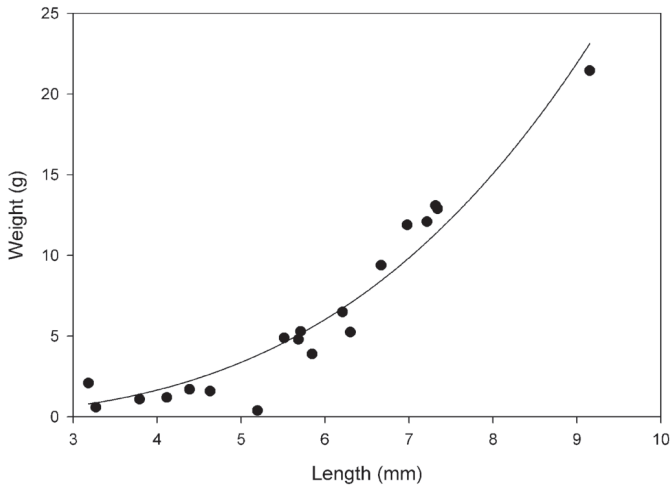


**Figure 9.** Relationship between angular length and total body weight.

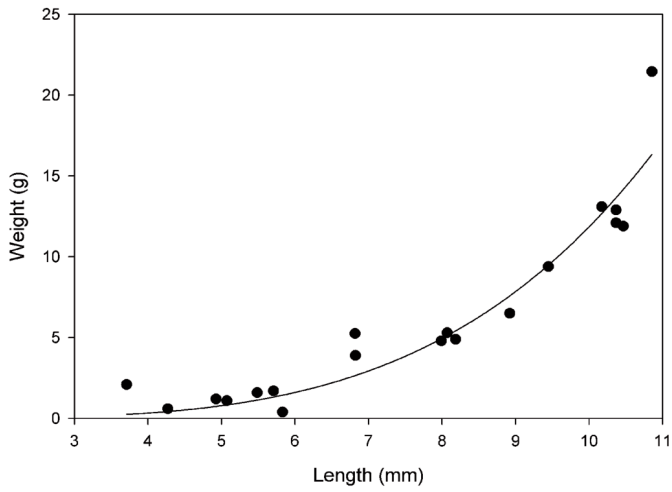


Figure 10. Relationship between maxilla length and total body weight.

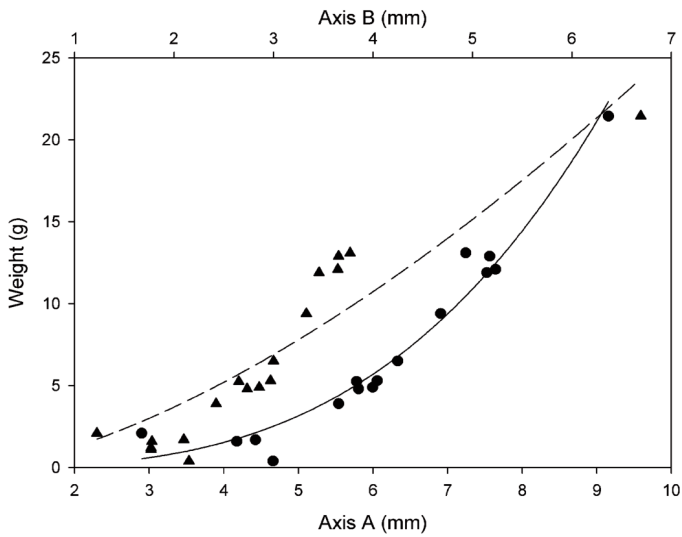


Figure 11. Relationships between hyomandibular axis lengths and total body weight. A – circles, solid curve; B – closed triangles, dashed curve.



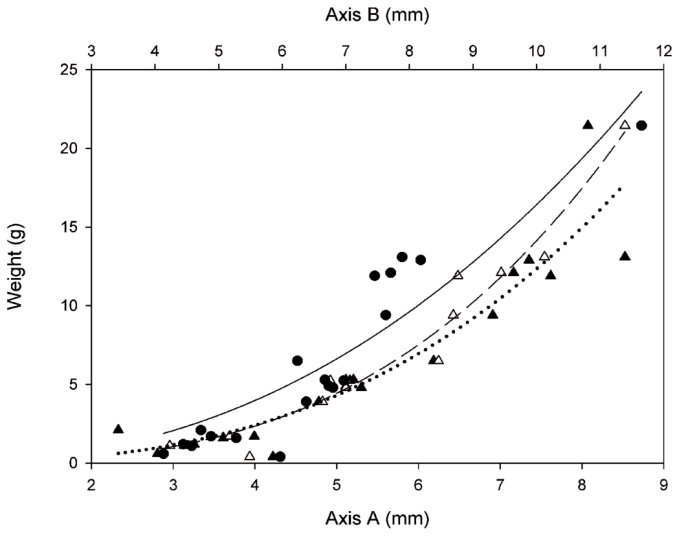


Figure 12. Relationships between preopercle axis lengths and total body weight. A – circles, solid curve; B (left) – closed triangles, dashed curve; B (right) – open triangles, dotted curve.

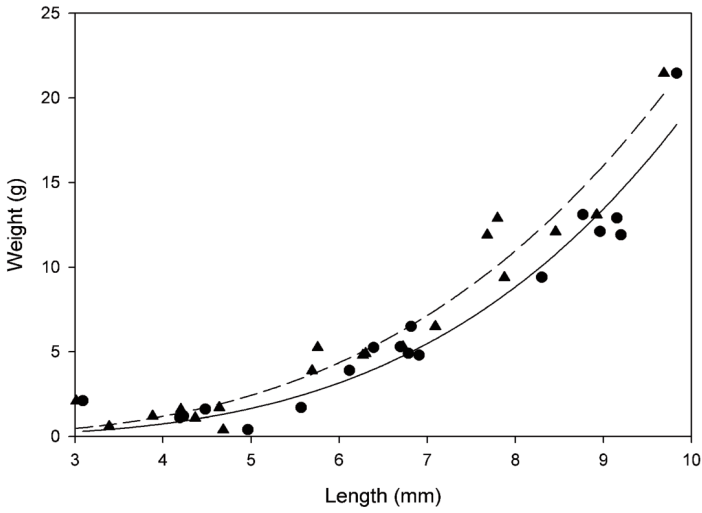
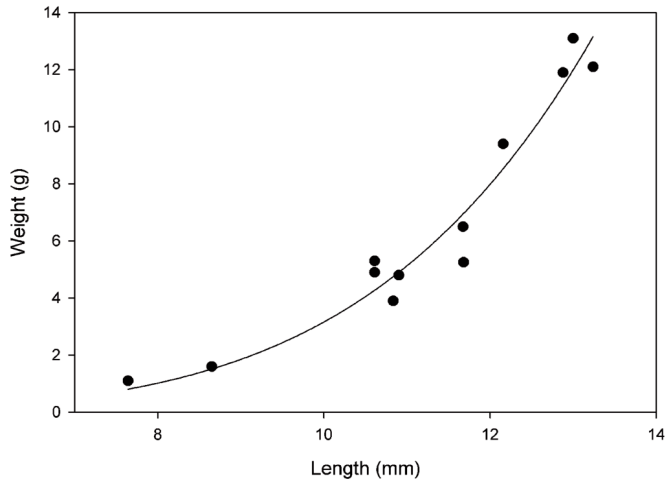


Figure 13. Relationships between opercle axis lengths and total body weight. A – circles, solid curve; B – closed triangles, dashed curve.



**Figure 14.** Relationship between parasphenoid axis A lengths and total body weight. Due to low descriptive power, the relationship for axis B is not shown.

## Relationships between the length of select head bones and body size for some Hawaiian parrotfishes (subfamily Scarinae)

KEN LONGENECKER (Hawaii Biological Survey, Bishop Museum, 1525 Bernice Street, Honolulu, Hawai'i 96817, USA; email: klongenecker@bishopmuseum.org), YVONNE CHAN & ERIK C. FRANKLIN (Hawai'i Institute of Marine Biology, University of Hawai'i, PO Box 1346, Kāne'ohe, Hawai'i 96744, USA)

Animal remains can be used to reconstruct patterns of resource use in dietary analysis and archaeology, and to reconstruct ancient environments in geology and paleontology. Estimating the body size of fishes from these remains is desirable, but rarely accomplished because the relationships between the size of a fish and its durable anatomical structures (e.g., bones) are largely unknown (Longenecker, 2008).

Parrotfishes form an important part of the diet of the critically endangered, endemic, Hawaiian monk seal diet (Goodman-Lowe, 1998; Longenecker *et al.*, 2006; Longenecker, 2010; Cahoon, 2011) and are a prominent fish component of Hawaiian archaeological deposits (Pearson *et al.*, 1971; Kirch, 1979, 1982; Goto, 1984; O'Day, 2001). Equations that allow total body size to be estimated from the size of parrotfish remains will help inform conservation decisions for an apparently food-limited marine mammal and lead to better understanding of prehistoric patterns of human resource exploitation in Hawai'i.

Here we present the results of regression analyses examining the relationship between the dimensions of select head bones and the total length and total body weight of Hawaiian scarine parrotfish specimens. The bones analyzed are those that have proven useful for identifying parrotfish remains (Longenecker *et al.*, 2006; Longenecker, 2010; Cahoon, 2011) and yield the highest estimates of minimum number of individuals in regurgitate and fecal samples of the Hawaiian monk seal and archaeological material from Nu'alolo Kai, Kaua'i (K1) and Wai'ahukini, Hawai'i (HA-B22-248, HA-B22-64). Axes chosen for measurement are those that are likely to persist after consumption and elimination, or deposition and excavation.

### Materials and Methods

Thawed, previously frozen specimens of the parrotfishes *Chlorurus perspicillatus* (Steindachner, 1879), *C. spilurus* (Valenciennes, 1840) (formerly *C. sordidus* (Forsskål, 1775)), and *Scarus dubius* Bennet, 1828 (nomenclature of Randall, 2007) collected from the Northwestern Hawaiian Islands in 2009 were measured (total, fork, and standard lengths) and weighed with a precision of 0.1 cm and 0.1 g, respectively. Heads, including the pharyngeal jaws, were removed, wrapped in aluminum foil, and exposed to low heat (~93°C) for 24 h to denature connective tissue. Oral and pharyngeal jaw bones were isolated, cleaned with stiff-bristled brushes, rinsed in fresh water, and air-dried at ~93°C.

Dimensions of these bones were measured with digital calipers. Images of the bones examined and axes measured are presented in Figures 1–14 (oral jaw bone terminology from Rojo, 1991; pharyngeal jaw bone terminology from Gobalet, 1989; all images from a 126 mm standard length specimen of *Chlorurus perspicillatus*). Regression analysis was used to describe the relationship between bone size and total length and total body weight.

Regression equations were constructed for all species individually, for all *Chlorurus* data combined, and for all species combined. For paired bones (premaxilla, maxilla, dentary, angular, maxilla, upper pharyngeal jaw), axes of both bones were measured and axis-length-to-total-length regressions for all species combined were compared with analysis of covariance. The mean of measurements from right and left bones from a single individual was used in regression analyses when no significant difference was detected between sides, otherwise side-specific equations were generated (e.g., premaxilla axis "A").

### Results and Discussion

Standard length can be modeled as a linear function of all bone axis lengths (Table 1) and total body weight can be predicted using a 2-parameter power function of all bone axis lengths (Table 2). Equations for all axes are listed from more- to less-inclusive taxonomic groups. The relationships for all data combined are based on members of the parrotfish subfamily Scarinae, represented in Hawai'i by the genera *Chlorurus* and *Scarus*. These equations should not be used for remains of *Calotomus*, which belong to the Sparisomatinae and have noticeably different dimensions of jaw bone axes.

These groupings serve three purposes. First, equations can be used to predict the size of a fish from remains larger or smaller than those used in the analyses. Although linear relationships with high coefficients of determination, such as many of those in Table 1, might reasonably be used for extrapolation, doing so with curvilinear relationships (Table 2) is likely to provide unrealistic estimates. Using a relationship for a higher taxon, based on a wider size range of individuals, may help avoid the need for extrapolation. Second, although molecular techniques make species-level identification of fish remains feasible, bones are more easily assigned to higher taxa. The groupings provide reasonable predictions of fish size when a species-level identification of parrotfish remains is not feasible. The more-general higher-taxa regressions should be used in such cases. Third, these groups also provide predictions for species not included in the analysis. With seven parrotfishes known from Hawai'i, the equations presented here represent a portion of the work necessary for detailed reconstruction of parrotfish assemblages. In the interim, these higher-taxa relationships may suffice for predicting the size of the remaining two Hawaiian members of the subfamily Scarinae (*Scarus psittacus* and *Scarus rubroviolaceus*).

### Acknowledgments

We thank the following people for their help: members of the ToBo lab at HIMB, especially Z. Szabo and M. Gaither, for their assistance with specimen collection; A. Dow, C. Fumar, and J. Leonard for assistance identifying, measuring, and weighing whole parrotfish specimens; and the Bishop Museum Department of Anthropology, especially R. Gard and T. Jiao, for access to archaeological specimens. This paper is a result of research funded by NOAA Coral Reef Conservation Grant NA09NMF4630123 to R.J. Toonen, T. Hunt, and D. Carlon. Specimen collection and processing were supported by National Marine Sanctuaries NWHICRER-HIMB partnership MOA-2005-008/6882. Images were produced using equipment funded by the National Science Foundation under Grant Number DEB 082868. Manuscript preparation/publication was supported by contract AB133F-06-CN-0139 with the Protected Species Division of the Pacific Islands Fisheries Science Center (NOAA/NMFS).

**Table 1. Regression coefficients for length estimates. Length = a + b(x) where x is the length of the axis measured.**

Bone – Axis (side)/Taxon	n	range (mm)	a	b	r <sup>2</sup>
Premaxilla – A (left)					
<i>Scarinae</i>	44	1.37 – 5.53	63.8681	62.1911	0.79
<i>Chlorurus</i>	34	1.37 – 5.53	41.2404	66.5384	0.82
<i>perspicillatus</i>	12	1.74 – 5.53	79.1995	62.8537	0.93
<i>spilurus</i>	22	1.37 – 4.58	61.8634	54.9123	0.69
<i>Scarus dubius</i>	10	1.41 – 3.52	24.1125	96.4955	0.97
Premaxilla – A (right)					
<i>Scarinae</i>	41	1.00 – 5.23	82.0082	62.1623	0.76
<i>Chlorurus</i>	33	1.26 – 5.23	61.8292	66.1964	0.79
<i>perspicillatus</i>	12	1.70 – 5.23	87.2212	65.2016	0.91
<i>spilurus</i>	21	1.26 – 4.51	88.7079	50.8398	0.61
<i>Scarus dubius</i>	8	1.00 – 3.29	67.3640	86.9705	0.94
Premaxilla – B					
<i>Scarinae</i>	38	1.56 – 6.77	62.5380	53.6031	0.77
<i>Chlorurus</i>	32	1.95 – 6.77	45.2705	56.1224	0.82
<i>perspicillatus</i>	12	2.19 – 6.77	80.6728	52.9736	0.98
<i>spilurus</i>	20	1.95 – 5.41	71.2681	44.3573	0.60
<i>Scarus dubius</i>	6	1.56 – 3.60	14.8120	86.7699	0.90
Maxilla – A					
<i>Scarinae</i>	41	2.36 – 9.07	81.3503	34.1696	0.75
<i>Chlorurus</i>	32	2.55 – 9.07	49.6754	37.9856	0.82
<i>perspicillatus</i>	12	3.04 – 9.07	64.3100	38.5789	0.95
<i>spilurus</i>	20	2.55 – 8.52	75.2878	30.6067	0.66
<i>Scarus dubius</i>	9	2.36 – 4.96	-14.8565	73.3997	0.97
Maxilla – B					
<i>Scarinae</i>	36	3.35 – 14.41	52.7680	24.6936	0.93
<i>Chlorurus</i>	30	3.35 – 14.41	49.9140	24.6055	0.94
<i>perspicillatus</i>	10	5.71 – 14.41	90.9364	21.9810	0.96
<i>spilurus</i>	20	3.35 – 12.19	53.3139	23.2969	0.93
<i>Scarus dubius</i>	6	5.38 – 9.96	-19.4396	37.5507	0.98
Dentary – A					
<i>Scarinae</i>	44	1.21 – 6.66	104.4707	44.5879	0.61
<i>Chlorurus</i>	35	1.83 – 6.66	75.0386	50.0696	0.66
<i>perspicillatus</i>	12	1.83 – 6.66	81.4597	56.0541	0.95
<i>spilurus</i>	23	1.83 – 5.50	111.9210	33.5923	0.42
<i>Scarus dubius</i>	9	1.21 – 3.13	58.0196	85.4702	0.88
Dentary – B					
<i>Scarinae</i>	37	1.21 – 6.05	99.2675	50.5028	0.62
<i>Chlorurus</i>	29	1.53 – 6.05	38.7314	63.6295	0.74
<i>perspicillatus</i>	11	2.25 – 6.05	76.2370	62.2758	0.97
<i>spilurus</i>	18	1.53 – 4.96	69.2207	47.9880	0.58
<i>Scarus dubius</i>	8	1.21 – 2.80	61.7226	97.7943	0.94
Angular – A					
<i>Scarinae</i>	29	4.81 – 14.21	-3.9974	27.7791	0.92
<i>Chlorurus</i>	25	4.81 – 14.21	-5.8451	27.6883	0.95
<i>perspicillatus</i>	7	8.97 – 14.21	59.0253	23.7270	0.99
<i>spilurus</i>	18	4.81 – 13.50	13.0110	24.8532	0.94
<i>Scarus dubius</i>	4	6.22 – 11.59	-30.8961	33.1060	0.99

<b>Table 1. Regression coefficients for length estimates (continued).</b>					
<b>Bone – Axis (side)/Taxon</b>	<b>n</b>	<b>range (mm)</b>	<b>a</b>	<b>b</b>	<b>r<sup>2</sup></b>
Angular – B					
Scarinae	29	1.70 – 6.60	40.0697	53.6614	0.80
<i>Chlorurus</i>	25	1.70 – 6.60	33.6170	54.0796	0.80
<i>perspicillatus</i>	7	3.75 – 6.43	97.0912	47.9287	0.93
<i>spilurus</i>	18	1.70 – 6.60	64.0733	43.0797	0.72
<i>Scarus dubius</i>	4	2.23 – 4.88	5.3739	72.4764	0.97
Upper Pharyngeal Jaw – A					
Scarinae	35	1.75 – 4.33	-20.7260	87.8946	0.87
<i>Chlorurus</i>	22	1.77 – 4.33	-23.7944	89.2257	0.87
<i>perspicillatus</i>	11	2.13 – 4.33	18.8367	79.6395	0.81
<i>spilurus</i>	11	1.77 – 3.84	-8.2536	77.6601	0.96
<i>Scarus dubius</i>	13	1.75 – 3.44	-7.3854	82.6310	0.90
Upper Pharyngeal Jaw – B					
Scarinae	35	3.88 – 11.03	17.9017	29.6919	0.92
<i>Chlorurus</i>	22	3.88 – 11.03	9.7368	30.4392	0.93
<i>perspicillatus</i>	11	4.73 – 11.03	49.1979	26.7023	0.92
<i>spilurus</i>	11	3.88 – 9.72	7.8577	29.1924	0.96
<i>Scarus dubius</i>	13	4.05 – 9.00	34.8713	27.8649	0.89
Upper Pharyngeal Jaw – C					
Scarinae	39	1.92 – 4.99	-2.7029	69.2349	0.95
<i>Chlorurus</i>	26	1.92 – 4.99	-472.0605	234.5373	0.92
<i>perspicillatus</i>	14	2.29 – 4.99	9.1790	66.7555	0.95
<i>spilurus</i>	12	1.92 – 3.86	-451.9630	231.0588	0.83
<i>Scarus dubius</i>	13	1.96 – 4.24	-316.4140	158.9411	0.72
Upper Pharyngeal Jaw – D					
Scarinae	39	2.39 – 6.17	-0.8470	54.0619	0.95
<i>Chlorurus</i>	26	2.48 – 6.17	-2.8453	54.2308	0.96
<i>perspicillatus</i>	14	2.91 – 6.17	15.0236	50.7321	0.96
<i>spilurus</i>	12	2.48 – 4.94	-26.2678	60.9749	0.92
<i>Scarus dubius</i>	13	2.39 – 5.43	0.4060	54.3868	0.88
Upper Pharyngeal Jaw – E					
Scarinae	39	1.49 – 3.92	1.0139	82.7888	0.90
<i>Chlorurus</i>	26	1.49 – 3.92	-0.5889	85.8921	0.93
<i>perspicillatus</i>	14	1.66 – 3.92	36.0357	75.6251	0.88
<i>spilurus</i>	12	1.49 – 3.40	-4.0370	84.7510	0.93
<i>Scarus dubius</i>	13	1.56 – 3.64	5.7966	76.3027	0.93
Lower Pharyngeal Jaw – A					
Scarinae	40	7.45 – 21.83	12.8485	14.2936	0.94
<i>Chlorurus</i>	27	8.41 – 21.83	11.3948	14.8167	0.97
<i>perspicillatus</i>	15	9.76 – 21.83	8.3607	14.8766	0.97
<i>spilurus</i>	12	8.41 – 17.76	-9.5808	16.8952	0.96
<i>Scarus dubius</i>	13	7.45 – 20.57	21.8879	12.8410	0.91
Lower Pharyngeal Jaw – B					
Scarinae	40	3.36 – 10.62	22.5257	29.3112	0.86
<i>Chlorurus</i>	27	3.56 – 10.62	16.5408	31.6758	0.94
<i>perspicillatus</i>	15	4.32 – 10.62	33.0558	29.9593	0.89
<i>spilurus</i>	12	3.56 – 8.66	22.8518	29.7368	0.93
<i>Scarus dubius</i>	13	3.36 – 9.97	24.3384	26.2671	0.87

**Table 2. Regression coefficients for weight estimates. Weight =  $a(x)^b$  where  $x$  is the length of the axis measured.**

Bone – Axis (side)/Taxon	n	range (mm)	a	b	r <sup>2</sup>
Premaxilla – A (left)					
<i>Scarinae</i>	44	1.37 – 5.53	23.2697	2.4214	0.82
<i>Chlorurus</i>	34	1.37 – 5.53	14.6851	2.7067	0.83
<i>perspicillatus</i>	12	1.74 – 5.53	53.2530	1.9564	0.87
<i>spilurus</i>	22	1.37 – 4.58	14.8484	2.5328	0.72
<i>Scarus dubius</i>	10	1.41 – 3.52	34.7862	2.5735	0.97
Premaxilla – A (right)					
<i>Scarinae</i>	41	1.00 – 5.23	43.3553	2.0954	0.76
<i>Chlorurus</i>	33	1.26 – 5.23	30.5914	2.3192	0.77
<i>perspicillatus</i>	12	1.70 – 5.23	45.6944	1.7779	0.81
<i>spilurus</i>	21	1.26 – 4.51	51.9503	1.6477	0.60
<i>Scarus dubius</i>	8	1.00 – 3.29	54.6344	2.3211	0.97
Premaxilla – B					
<i>Scarinae</i>	38	1.56 – 6.77	14.8559	2.4634	0.85
<i>Chlorurus</i>	32	1.95 – 6.77	8.2015	2.7976	0.89
<i>perspicillatus</i>	12	2.19 – 6.77	26.6599	2.1696	0.98
<i>spilurus</i>	20	1.95 – 5.41	18.4843	2.0999	0.65
<i>Scarus dubius</i>	6	1.56 – 3.60	10.6914	3.2881	0.89
Maxilla – A					
<i>Scarinae</i>	41	2.36 – 9.07	10.6194	2.1706	0.78
<i>Chlorurus</i>	32	2.55 – 9.07	5.1838	2.5081	0.83
<i>perspicillatus</i>	12	3.04 – 9.07	8.1747	2.3520	0.90
<i>spilurus</i>	20	2.55 – 8.52	12.1256	1.9331	0.74
<i>Scarus dubius</i>	9	2.36 – 4.96	3.7359	3.3953	0.99
Maxilla – B					
<i>Scarinae</i>	36	3.35 – 14.41	3.6371	2.1992	0.91
<i>Chlorurus</i>	30	3.35 – 14.41	3.2052	2.2444	0.92
<i>perspicillatus</i>	10	5.71 – 14.41	11.6277	1.7704	0.94
<i>spilurus</i>	20	3.35 – 12.19	3.8454	2.1021	0.93
<i>Scarus dubius</i>	6	5.38 – 9.96	0.2663	3.5126	0.96
Dentary – A					
<i>Scarinae</i>	44	1.21 – 6.66	21.3630	2.2703	0.71
<i>Chlorurus</i>	35	1.83 – 6.66	9.9770	2.7172	0.76
<i>perspicillatus</i>	12	1.83 – 6.66	35.7891	2.0724	0.97
<i>spilurus</i>	23	1.83 – 5.50	27.1425	1.8443	0.50
<i>Scarus dubius</i>	9	1.21 – 3.13	54.0454	2.2024	0.76
Dentary – B					
<i>Scarinae</i>	37	1.21 – 6.05	21.9067	2.3927	0.72
<i>Chlorurus</i>	29	1.53 – 6.05	10.2689	2.8606	0.80
<i>perspicillatus</i>	11	2.25 – 6.05	39.9453	2.1171	0.99
<i>spilurus</i>	18	1.53 – 4.96	18.1491	2.2381	0.58
<i>Scarus dubius</i>	8	1.21 – 2.80	47.8149	2.7166	0.93
Angular – A					
<i>Scarinae</i>	29	4.81 – 14.21	0.5871	2.8713	0.92
<i>Chlorurus</i>	25	4.81 – 14.21	0.4084	3.0061	0.93
<i>perspicillatus</i>	7	8.97 – 14.21	5.7049	2.0269	0.97
<i>spilurus</i>	18	4.81 – 13.50	0.7423	2.6969	0.93
<i>Scarus dubius</i>	4	6.22 – 11.59	0.3671	3.1706	0.99

**Table 2. Regression coefficients for weight estimates (continued).**

<b>Bone – Axis (side)/Taxon</b>	<b>n</b>	<b>range (mm)</b>	<b>a</b>	<b>b</b>	<b>r<sup>2</sup></b>
Angular – B					
<i>Scarinae</i>	29	1.70 – 6.60	13.7192	2.3867	0.78
<i>Chlorurus</i>	25	1.70 – 6.60	10.1742	2.5459	0.79
<i>perspicillatus</i>	7	3.75 – 6.43	53.5363	1.7137	0.93
<i>spilurus</i>	18	1.70 – 6.60	13.6168	2.2006	0.73
<i>Scarus dubius</i>	4	2.23 – 4.88	15.3422	2.5585	0.97
Upper Pharyngeal Jaw – A					
<i>Scarinae</i>	35	1.75 – 4.33	13.1703	2.8277	0.78
<i>Chlorurus</i>	22	1.77 – 4.33	18.2429	2.6159	0.80
<i>perspicillatus</i>	11	2.13 – 4.33	41.3543	2.0310	0.72
<i>spilurus</i>	11	1.77 – 3.84	5.4490	3.4687	0.99
<i>Scarus dubius</i>	13	1.75 – 3.44	11.3677	2.8017	0.80
Upper Pharyngeal Jaw – B					
<i>Scarinae</i>	35	3.88 – 11.03	1.1265	2.7358	0.94
<i>Chlorurus</i>	22	3.88 – 11.03	1.3627	2.6606	0.96
<i>perspicillatus</i>	11	4.73 – 11.03	3.7875	2.2186	0.93
<i>spilurus</i>	11	3.88 – 9.72	0.4186	3.1854	0.99
<i>Scarus dubius</i>	13	4.05 – 9.00	2.0075	2.4121	0.92
Upper Pharyngeal Jaw – C					
<i>Scarinae</i>	39	1.92 – 4.99	6.5528	2.9831	0.90
<i>Chlorurus</i>	26	1.92 – 4.99	10.1078	2.7149	0.93
<i>perspicillatus</i>	14	2.29 – 4.99	11.2867	2.6303	0.92
<i>spilurus</i>	12	1.92 – 3.86	2.2183	4.0551	0.95
<i>Scarus dubius</i>	13	1.96 – 4.24	6.3516	2.8706	0.74
Upper Pharyngeal Jaw – D					
<i>Scarinae</i>	39	2.39 – 6.17	3.8308	2.8686	0.93
<i>Chlorurus</i>	26	2.48 – 6.17	4.8084	2.7473	0.94
<i>perspicillatus</i>	14	2.91 – 6.17	5.5553	2.6547	0.95
<i>spilurus</i>	12	2.48 – 4.94	0.4697	4.4321	0.97
<i>Scarus dubius</i>	13	2.39 – 5.43	4.8862	2.6431	0.79
Upper Pharyngeal Jaw – E					
<i>Scarinae</i>	39	1.49 – 3.92	9.1431	3.1969	0.83
<i>Chlorurus</i>	26	1.49 – 3.92	16.6609	2.7883	0.90
<i>perspicillatus</i>	14	1.66 – 3.92	28.1701	2.3688	0.83
<i>spilurus</i>	12	1.49 – 3.40	6.8825	3.6158	0.97
<i>Scarus dubius</i>	13	1.56 – 3.64	7.5385	3.1133	0.89
Lower Pharyngeal Jaw – A					
<i>Scarinae</i>	40	7.45 – 21.83	0.0691	2.9937	0.88
<i>Chlorurus</i>	27	8.41 – 21.83	0.1865	2.6882	0.96
<i>perspicillatus</i>	15	9.76 – 21.83	0.1335	2.7935	0.96
<i>spilurus</i>	12	8.41 – 17.76	0.0276	3.4576	0.98
<i>Scarus dubius</i>	13	7.45 – 20.57	0.0875	2.8091	0.90
Lower Pharyngeal Jaw – B					
<i>Scarinae</i>	40	3.36 – 10.62	1.1706	2.7365	0.76
<i>Chlorurus</i>	27	3.56 – 10.62	2.2679	2.5009	0.89
<i>perspicillatus</i>	15	4.32 – 10.62	4.2811	2.2116	0.81
<i>spilurus</i>	12	3.56 – 8.66	0.4647	3.2811	0.96
<i>Scarus dubius</i>	13	3.36 – 9.97	0.6431	2.8360	0.85



**Literature Cited**

- Cahoon, M.K.** 2011. *The Foraging Ecology of Monk Seals in the Main Hawaiian Islands*. MS Thesis. University of Hawai'i at Mānoa, Honolulu. 172p.
- Gobalet, K.W.** 1989. Morphology of the parrotfish pharyngeal jaw apparatus. *American Zoologist* **29**: 319-331.
- Goodman-Lowe, G.** 1998. Diet of Hawaiian monk seal (*Monachus schauinslandi*) from the Northwestern Hawaiian Islands during 1991-1994. *Marine Biology* **132**: 535-546.
- Goto, A.** 1984. Marine exploitation at South Point, Hawai'i Island: an aspect of adaptive diversity in Hawaiian prehistory. *Hawaiian Archaeology* **1**:44-63.
- Kirch, P.V.** 1979. Marine exploitation in prehistoric Hawai'i: archaeological investigations at Kalāhipua'a, Hawai'i Island. *Pacific Anthropological Records* **29**. Bishop Museum, Honolulu. 235p.
- . 1982. The ecology of marine exploitation in prehistoric Hawaii. *Human Ecology* **10**: 455-476.
- Longenecker, K.** 2008. Relationships between otolith size and body size for Hawaiian reef fishes. *Pacific Science* **62**: 533–39.
- . 2010. Fishes in the Hawaiian monk seal diet, based on regurgitate samples collected in the Northwestern Hawaiian Islands. *Marine Mammal Science* **26**: 420-29.
- , **Dollar, R.A., Cahoon, M.** 2006. Increasing taxonomic resolution in dietary analysis of the Hawaiian monk seal. *Atoll Research Bulletin* **543**:103-113.
- O'Day, S.J.** 2001. Excavations at the Kipapa Rockshelter, Kahikinui, Maui, Hawai'i. *Asian Perspectives* **40**: 279-304.
- Pearson, R., Kirch, P.V. & Pietrusewsky, M.** 1971. An early prehistoric site at Bellows Beach, Waimanalo, Oahu, Hawaiian Islands. *Archaeology and Physical Anthropology in Oceania* **6**: 204-234.
- Randall, J.E.** 2007. *Reef and Shore Fishes of the Hawaiian Islands*. University of Hawai'i Sea Grant College Program, Honolulu. 546p.
- Rojo, A.L.** 1991. *Dictionary of Evolutionary Fish Osteology*. CRC Press, Boca Raton. 273p.

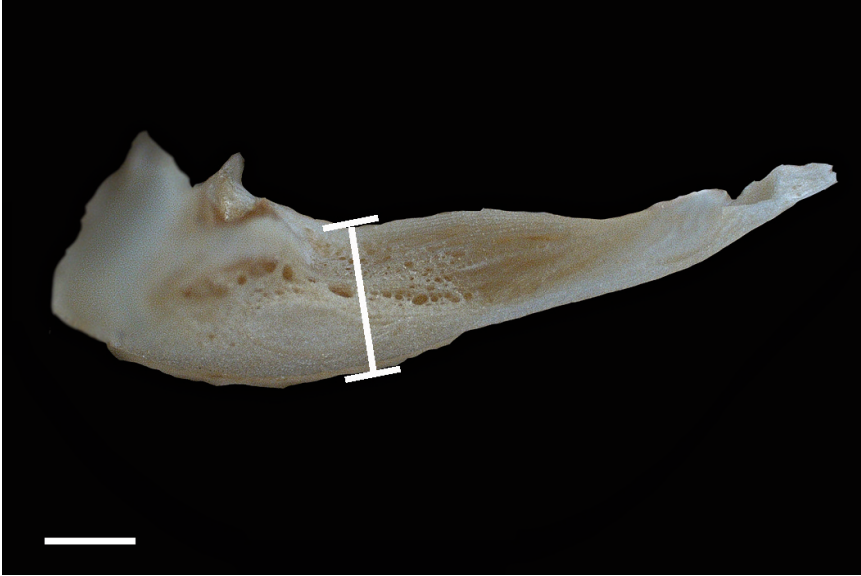


**Figure 1.** Axis A of premaxilla (dorsal aspect). Minimum width of posterior to ascending process (jaws of calipers held parallel to ascending process). Scale bar = 1 mm.



**Figure 2.** Axis B of premaxilla (medial aspect, rotated 90° clockwise from its normal anatomical position). Width of ascending process at constriction. Scale bar = 1 mm.



**Figure 3.** Axis A of maxilla (ventral aspect). Shortest distance between indentations on internal and external processes. Scale bar = 1 mm.



**Figure 4.** Axis B of maxilla (medial aspect). Maximum distance along internal process. Scale bar = 1 mm.

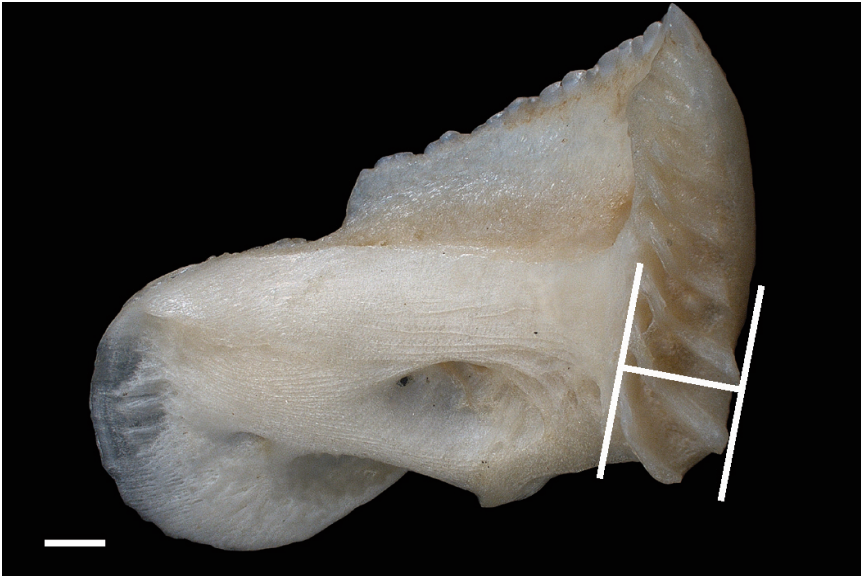


**Figure 5.** Axis A of dentary (lateral aspect). Maximum distance across interdigitating flanges of mandibular symphysis (jaws of calipers held parallel to posterior edge of flanges at their greatest width). Scale bar = 1 mm.

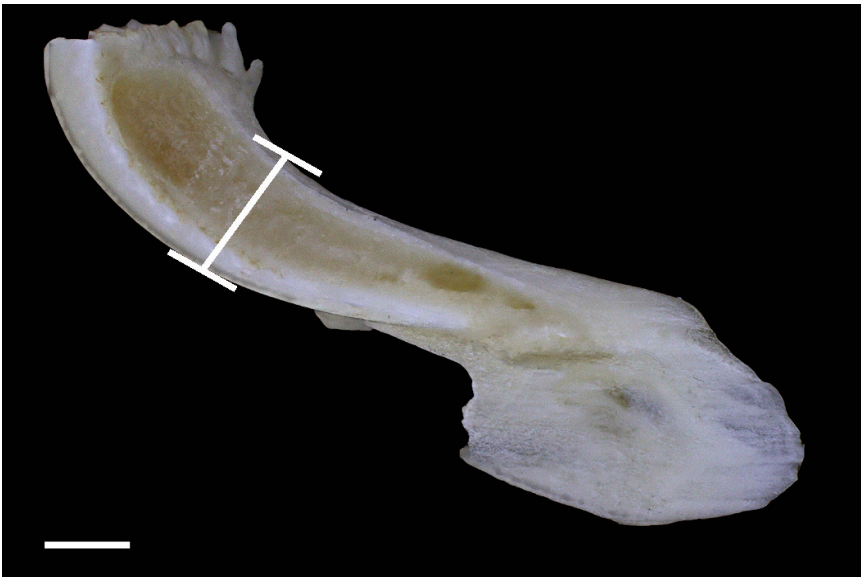


**Figure 6.** Axis B of dentary (dorsal aspect). Shortest width at point of maximum inflection (jaws of calipers held parallel to lateral face of bone). Scale bar = 1 mm.



**Figure 7.** Axis A of angular (medial aspect, right bone). Shortest distance between terminus of anterior process and quadrate facet. Scale bar = 1 mm.

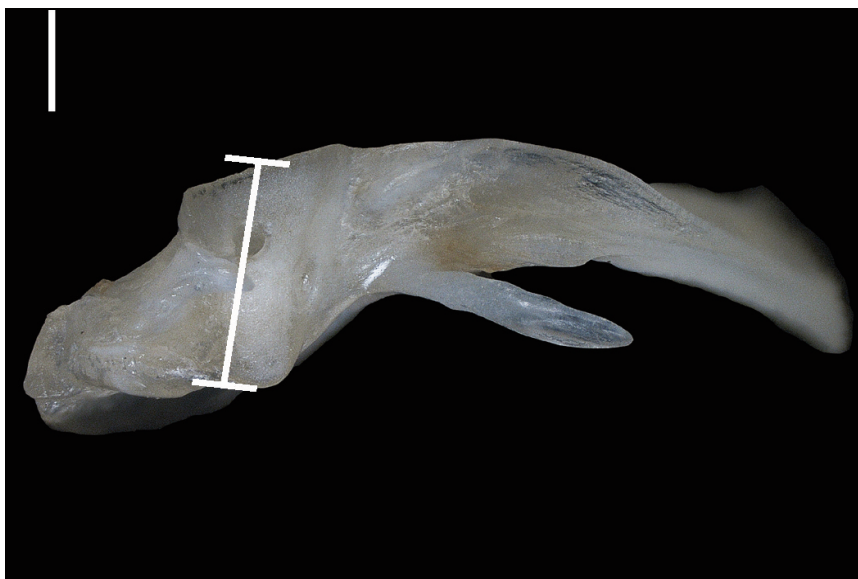


**Figure 8.** Axis B of angular (posterior aspect, right bone, rotated 90° clockwise from its normal anatomical position). Distance across deepest area of quadrate facet. Scale bar = 1 mm.

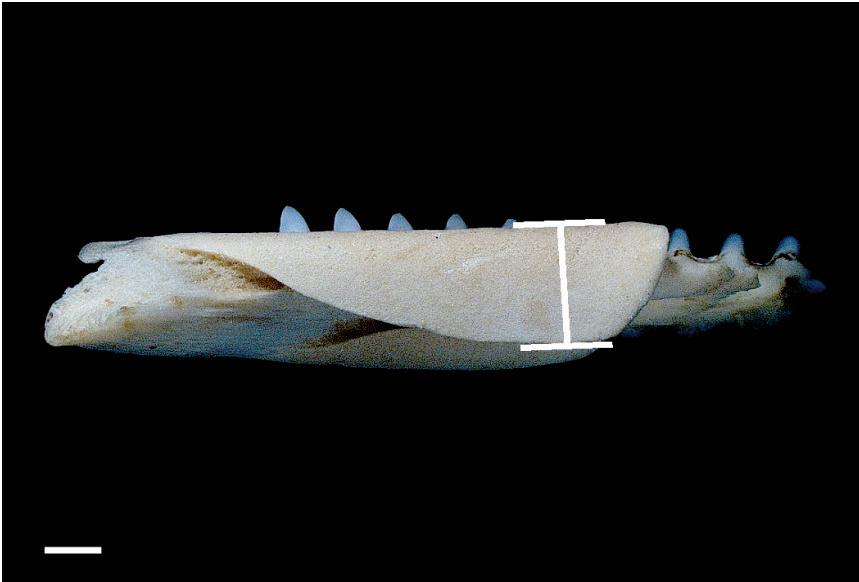


**Figure 9.** Axis A of upper pharyngeal jaw (dorsal aspect). Greatest width of cranial condyle (jaws of calipers held parallel to medial border). Scale bar = 1 mm.



**Figure 10.** Axis B of upper pharyngeal jaw (lateral aspect). Width between fourth-epibranchial condyle and cranial condyle (jaws of calipers held parallel to articulating face of cranial condyle, with tip of one jaw at posterior end of fourth-epibranchial condyle). Scale bar = 1 mm.



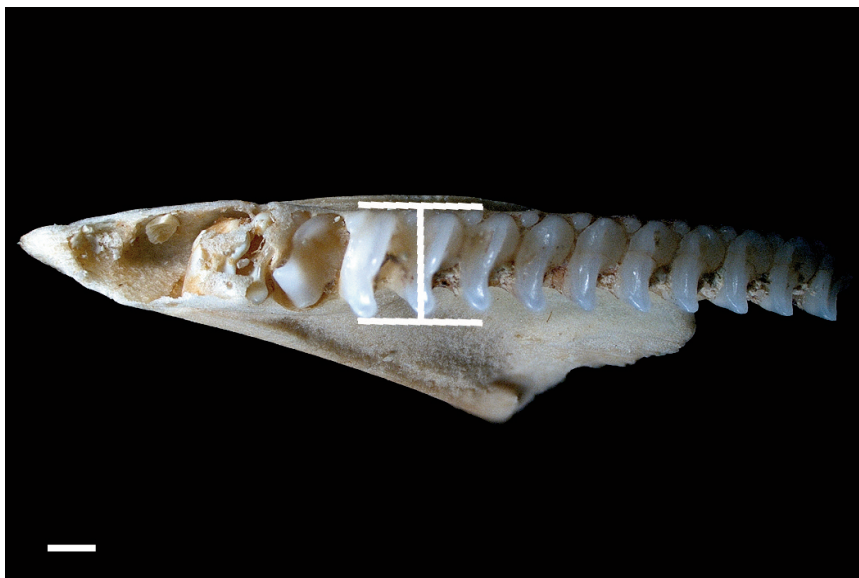


**Figure 11.** Axis C of upper pharyngeal jaw (ventral aspect). Width of anterior-most teeth (jaws of calipers held parallel to lateral edge of teeth). Scale bar = 1 mm.



**Figure 12.** Axis D of upper pharyngeal jaw (posterior aspect). Width at lateral extreme of fourth-epibranchial condyle when medial face of body is held vertically. Scale bar = 1 mm.



**Figure 13.** Axis E of upper pharyngeal jaw (anterior aspect). Width at base of anterior teeth (anterior portion of bone removed for illustrative purpose). Scale bar = 1 mm.

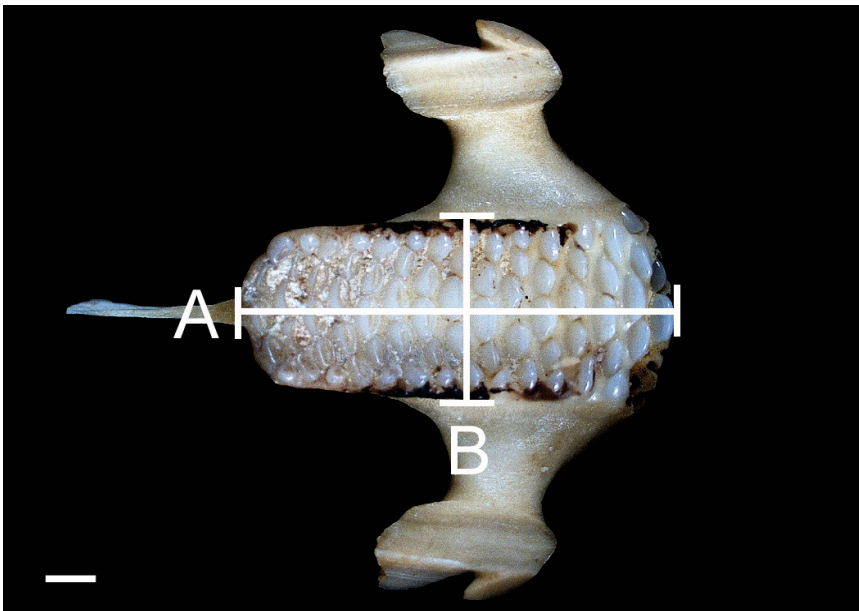


**Figure 14.** Axes of lower pharyngeal jaw (dorsal aspect). A – maximum length of tooth plate; B – maximum width of tooth plate. Scale bar = 1 mm.





## Tools for Reconstructing Hawaiian Fish Assemblages

---

### Table of Contents

Preface .....	1
Relationships between the length of select head bones and body weight for <i>Pseudanthias</i> (Serranidae: Anthiinae), numerically important prey of the endangered Hawaiian monk seal — Longenecker, K. . . .	3
Relationships between the length of select head bones and body size for some Hawaiian parrotfishes (subfamily Scarinae) — Longenecker, K., Chan, Y. & Franklin, E.C. ....	13

---